Efficiency Evaluation of Six-Phase VSI and NSI for 400V and 800V Electric Vehicle Powertrains

Saif Absar, Wesam Taha, and Ali Emadi
McMaster Automotive Resource Centre (MARC)
McMaster University
Hamilton, ON, Canada
{absars1, tahaw, emadi}@mcmaster.ca

IECON 2021 - 47th Annual Conference of the IEEE Industrial Electronics Society | 978-1-6654-3554-3/21/$31.00 ©2021 IEEE | DOI: 10.1109/IECON48115.2021.9589939

***Abstract*—This paper presents an efficiency evaluation of two six-phase inverter topologies for automotive applications: voltage source inverter (VSI) and nine-switch inverter (NSI). Their efficiency is studied for electric powertrains rated at 400 V and 800 V, and using silicon carbide (SiC) MOSFETs rated at 650 V and 1200 V operating at a switching frequency of 30 kHz. Prior to efficiency evaluation, a thorough analysis on the total device count required for 100 kW design is investigated for both topologies. It is found that NSI enjoys a superior efficiency when compared to six-phase VSI, at the expense of increased total device count.**

***Index Terms*—electric vehicle, multiphase drives, power converters, silicon carbide, vehicular technology**

I. Introduction

Recent years have witnessed an uptake of electrification in all sectors of transportation [1]. Driven by the need for eco-friendly solutions, this trend is only expected to grow in the future. More than half of the global sales of passenger vehicles is expected to be electric by 2040 [2]. However, to meet the expected demand, electrified transportation must develop further in order to become a sustainable, inexpensive and reliable technology [3]. As such, extensive research and development efforts are being spent to bridge the technology gap on all fronts.

On the electric traction drive system front, multiphase drives (MPDs) have garnered a lot of attention lately [4]. MPDs offer a multitude of advantages including lower torque pulsation, reduced per-phase current handling, and enhanced fault tolerance [5]. They are well suited for reliability-stringent applications such as more electric aircrafts (MEA) [6] and high power/high torque applications like heavy-duty vehicles [7]. Currently, six-phase drives stand as the best choice for MPDs for automotive applications, owing to the tradeoff between modularity and fault tolerance from one end, and cost and complexity from the other end [4]. This is trend is also aided by the rise of wide bandgap (WBG) devices, especially silicon carbide (SiC) [8]. SiC MOSFETs have demonstrated a multitude of advantages over silicon (Si) IGBTs, namely higher breakdown voltages, higher switching frequencies, higher operating temperatures, smaller on-state resistances, and chip size reduction [9].

From the inverter side, the six-phase inverter can be built by extending the conventional two-level, three-phase voltage source inverter (VSI) to include six switching poles, as depicted in Fig. 1a. Alternatively, six-phase machines can be driven by a nine-switch inverter (NSI), shown in Fig. 1b. The NSI utilizes three switches per leg, with each leg supplying two phases. As the name suggests, the prominent advantage of NSI is the reduced switch count when compared to the six-phase VSI. The utilization of NSI has been investigated for various applications including ac-ac power conversion [10], uninterruptible power supplies [11], and hybrid electric vehicles (EVs) [12].

On the other hand, the reduced switch count in NSI comes at the expense of reduced fault tolerance capability when compared to its VSI counterpart. An open-circuit fault in one switch yields the loss of two machine phases [13]. Additionally, a NSI with fourth leg (of three switches) was proposed in [14] to cope with unbalanced loads. Yet, it mostly criticized for its low powertrain utilization [4]. When compared to the six-phase VSI, the NSI requires 20% and 33% higher dc-link voltage to produce the same output power, when the winding of the machine is in asymmetrical and symmetrical configurations, respectively [15].

Many NSI modulation techniques have been proposed in literature to address its aforementioned shortcomings [16]–[18]. An equivalent modulation mechanism linking NSI to six-phase VSI was devised in [19]. However, a thorough efficiency evaluation of the NSI, and its benchmark against VSI, has not been reported. In [10], simulation results demonstrated a superior efficiency by NSI over VSI using Si IGBTs. However, it was found that the switching loss profile of the NSI, operating in common frequency (CF) mode, is not evenly distributed among the devices. A current peak tracking technique was proposed in [20] to reduce the switching loss of NSI and achieve a balanced loss profile. As of this writing, the employment of SiC devices in NSI has not been explored. Furthermore, while NSI enjoys a reduced switch count, the total number of employed devices is not necessarily lower when compared to VSI—a fact somewhat overlooked in previous studies. Since each leg in NSI supplies two windings of the six-phase machine, the employed switching device must be rated to withstand double the current rating of its counterpart in VSI. To this end, the present paper contributes to existing knowledge in twofold: 1) the selection of SiC MOSFETs in six-phase NSI and VSI for different powertrain ratings 2) comprehensive efficiency comparison between the two topologies.

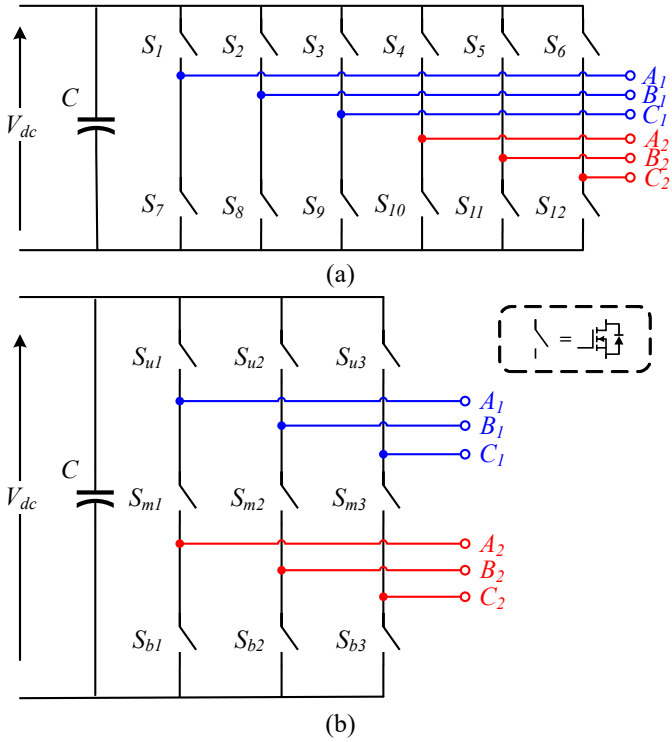

Fig. 1. Six-phase inverter topologies. (a) VSI. (b) NSI (subscripts u, m, and b denote upper, middle, and bottom, respectively).

II. Inverter Topologies and Modulation

This section reviews the topology and modulation scheme of the two six-phase inverter topologies studied in this paper. The total number of required devices in both topologies is also investigated, assuming SiC MOSFET switches.

A. Topology Overview

The conventional three-phase VSI is the automotive-industry-accepted topology, owing to its simplicity, low cost and high efficiency [21]. The six-phase VSI (Fig. 1a) employs an additional three phase legs with twelve switches in total. Paradoxically, the higher total switch count in the six-phase VSI, does not necessarily mean an increase in the total device count. This is particularly true for SiC-based high-power inverters where device paralleling is implemented to overcome the current limitation of the semiconductor devices. For instance, Tesla's Model 3 (2018) employs *four* SiC MOSFETs in parallel per switch position to handle the per-phase rated current (24 devices total) [22]. In six-phase VSI the per-phase current is half of its three-phase counterpart. So, if Tesla's Model 3 inverter were to be implemented in six-phase configuration, only *two* devices in parallel would be required. Thus, the total number of devices in the six-phase VSI is equal to its three-phase counterpart (2 devices per each of the 12 switches). Therefore, multiphase VSI alleviates current balancing issues among the paralleled devices [23]. On the other hand, increased cost is expected from gate drivers. Furthermore, six-phase VSI enjoys 10% volume reduction in DC-bus capacitor [24].

The NSI (Fig. 1b) was originally conceived to independently drive two three-phase machines [25], and later adopted for six-phase drives. It is composed of three legs, with three switches per leg, namely the upper, middle, and bottom switch, denoted S_u, S_m, and S_b, respectively. The two three-phase sets can either be driven at a common frequency (CF) or different frequency (DF). For six-phase applications, only CF mode is employed. While NSI is usually promoted for its lower switch count, the total number of devices could be higher when compared to six-phase VSI, for the same power rating. This is because the per-leg current rating is similar to that of the three-phase VSI, since each leg in NSI carries two phase currents. Thus, a higher current stress is experienced by the devices in the NSI when compared to switches in the VSI. To further illustrate this, Fig. 3 compares the minimum number of paralleled devices per switch position in both topologies and the resulting total number of devices. The minimum number of devices is computed based on the output phase current as a function of device rated current. For output current between one to two times the device rated current, VSI requires one device per switch position. On the other hand, NSI requires two devices to be paralleled per switch position. This yields a total number of required devices in NSI that is 1.2 times higher its VSI counterpart. For quadruple the device rated current, the increase in the total number of devices in NSI is 50%. While it is trivial for a designer to choose a device whose rated current is higher than the inverter output current (i.e. green region in Fig. 2b), the market availability may be limited. The maximum current rating of state of the art SiC MOSFETs is around 100 A [26]. Such a limitation calls for multiple devices paralleling per switch position. More often than not, this is the case for automotive traction inverters rated at $\geq$100 kW, as will be demonstrated in Section III.

B. Modulation Scheme

Sinusoidal PWM (SPWM) is adopted in this paper to study the efficiencies of the two inverter topologies in Fig. 1. The SPWM scheme for the NSI is depicted in Fig. 3. Each of the two three-phase sets has a modulation index associated with: m_u and m_b for upper and bottom switches, respectively. Each leg has two level-shifted reference sinusoidal signal, factored by the modulation index with a positive and negative offset for the upper and lower devices, respectively. For six-phase loads, the offset value is the same for both three phase sets and $m_u = m_l$ in order to produce a balanced output. In this study, the offset is set to 0.2. The resulting reference signals are compared to a triangular carrier to generate the gating pulses for S_u and S_b. Gating pulses for S_m are generated using an XOR logic gate of the upper and lower gate signals to prevent a leg short circuit. The maximum modulation index for NSI is defined as:

$$M_{max} = 1/(1 + sin(\theta/2)) \quad (1)$$

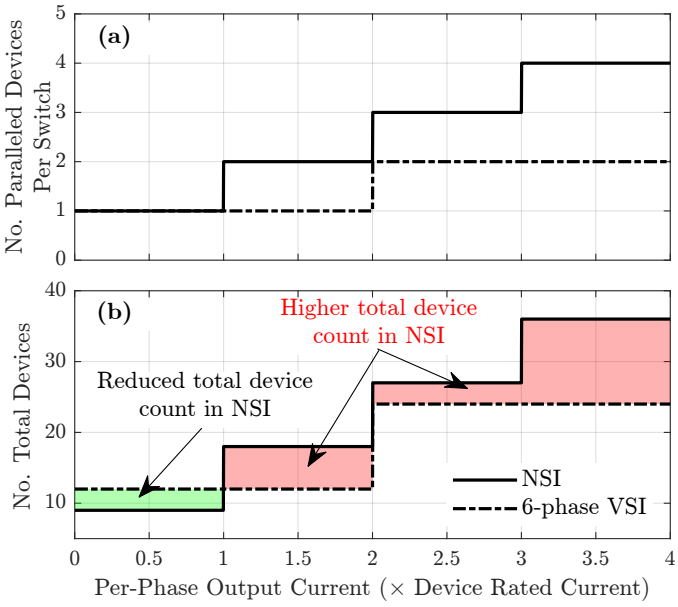

Fig. 2. Number of devices needed in six-phase VSI and NSI as a function of per-phase output current at a fixed DC-link voltage. (a) Number of paralleled devices per switch position. (b) Total device count per inverter topology.

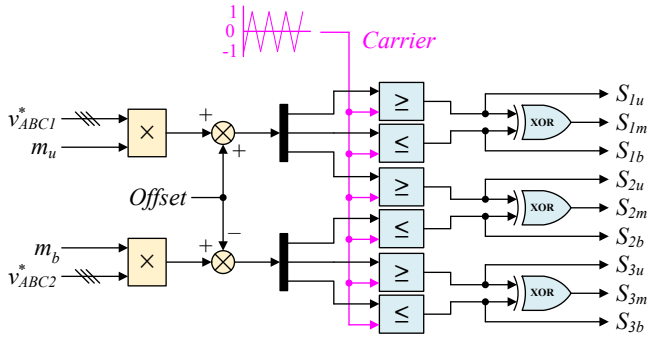

Fig. 3. SPWM control scheme for the NSI in Fig. 1b. m_u and m_b are the modulation indices for the upper and bottom winding sets, respectively.

where θ is the phase displacement angle between the two three-phase sets. For asymmetrical machine/load, $\theta = 30°$. Thus, $M_{max} \approx 0.8$.

III. Device Selection and Inverter Efficiency

A 100 kW design is considered for the two six-phase inverter topologies in Fig. 1. Their efficiency is evaluated for EV traction applications for two powertrain voltages: 400 V and 800 V. The most commonly used device voltage for a 400 V and 800 V powertrains are 650 V and 1200 V, respectively [27]. Accordingly, this study utilizes discrete SiC MOSFETs from Cree of the rating 650V/97A and 1200V/115A as listed in Table I. The SiC MOSFETs have been employed as bidirectional switches in the study. Hence, no anti-parallel diodes are used. Efficiency evaluation of both topologies is studied in two different cases:

- Case A: minimum number of device count;
- Case B: same number of total device count, with uneven paralleling in NSI at 800V.

Table II summarizes the total device count for each of the topologies in each case. The details of each case, along with efficiency investigation, is detailed next.

A. Inverter Efficiency

Inverter efficiency of the two topologies, employing the devices listed in Table I, is studied over load current sweep. Conduction and switching losses are evaluated in PLECS based on the thermal model of the devices provided by the manufacturer. The switching frequency is 30 kHz, the device junction temperature is fixed at a $T_j = 120$ °C, the modulation index is fixed at $m_a = 0.8$, and the power factor (PF) is 0.9. The dc-link is modeled by an ideal voltage source.

1) Case A: The minimum device count per switch position with respect to current ratings for the two inverters is two devices for the VSI and four devices for NSI at 400 V. For 800 V powertrain, one device (i.e. no paralleling) for the VSI and two devices for NSI at 800 V. The total device count is 24 and 36 for VSI and NSI respectively, at 400 V. Similarly, at 800 V the total device count is 12 and 18 for VSI and NSI, respectively. The efficiency of the two inverters is shown in Fig. 4 while the load current is swept from 0.1 to 1.0 pu. In Fig. 4a, a higher efficiency for NSI is observed throughout the load range for the 400 V powertrain. At 1 pu load current, the efficiency of the NSI is higher than the VSI by 0.5%. Similarly for the 800 V powertrain (Fig. 4b), the NSI obtains higher efficiency throughout the load range, with a gain of 0.75% at 1.0 pu load current. Therefore, when designed for the least number of devices NSI offers higher efficiency over VSI at the 400 and 800 V bus respectively, at the expense of six to twelve additional devices. Beyond 0.6 pu, the increase in efficiency in NSI becomes more prominent. To further analyze the steep efficiency drop in VSI in Fig. 4b beyond 0.6 pu, the difference in switching loss around 0.6 pu load current is illustrated in Fig. 5a. It is noted that although conduction loss, in both NSI and VSI, increase linearly with load current increase, the switching loss increase is non-linear in VSI beyond 0.6 pu.

TABLE I
EMPLOYED SiC DEVICES FOR 400 V AND 800 V EV POWERTRAINS

Powertrain	Part Number	Voltage (V)	Current (A)
400 V	C3M0025065D	650	97
800 V	C3M0016120D	1200	115

TABLE II
COMPARISON BETWEEN THE STUDIED CASES IN TERMS OF TOTAL DEVICE COUNT AND RELATIVE EFFICIENCY

Case	Inverter Topology	Device Count 400V	Device Count 800V	Efficiency
A	VSI	24	12	Low
	NSI	36	18	Medium
B	VSI	36	24	High
	NSI	36	24	High

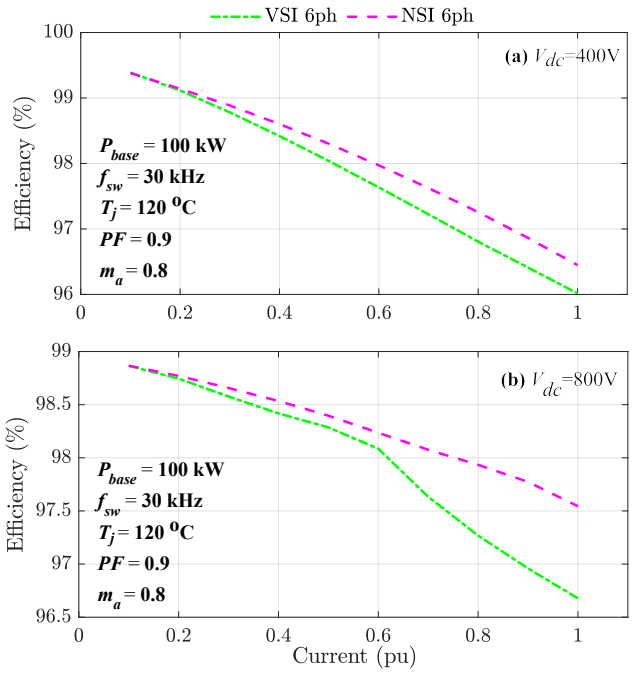

Fig. 4. Inverter efficiency evaluation with minimum device count vs. load current sweep. (a) 400 Vdc. (b) 800 Vdc.

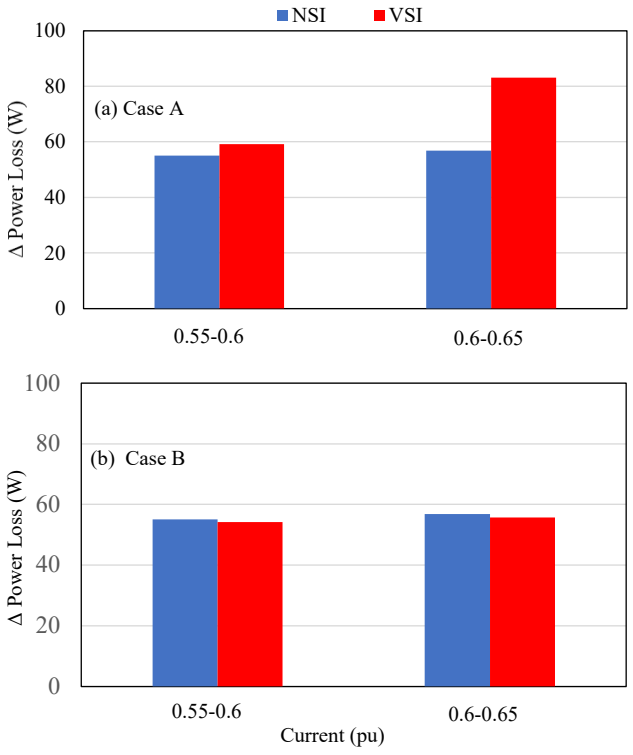

Fig. 5. Switching loss difference around 0.6 pu load current at 800 Vdc. (a) Case A. (b) Case B.

2) Case B: This evaluation was performed to draw inference on the following:

- To gauge the efficiency of the VSI and NSI employing the same number of total devices, with a total device count of 36 and 24 for VSI and NSI at 400 V and 800 V, respectively.
- To understand the non-linear increase in switching loss at 0.6 pu for VSI at 800 V.
- To investigate the possibility of utilizing uneven device distribution per switch position in NSI to achieve uniform power loss.

The efficiency of the two inverters employing the same total number of device count is depicted in Fig. 4 while the load current is swept from 0.1 to 1.0 pu. For the 400 V powertrain (Fig. 6a), the VSI consistently outperforms the NSI in terms of efficiency. At 1.0 pu, the VSI is higher in efficiency when compared to the NSI by almost 1%. On the other hand, for the 800 V powertrain (Fig. 6b), VSI has a higher efficiency only beyond 0.7 pu load current.

Testing under the same aforementioned conditions, it is observed in Fig. 5b that the increase in switching loss is linear from 0.6 pu to 0.65 pu. Furthermore, the switching loss in VSI is slightly lower when compared to NSI. This is attributed to the lower device current in VSI with two paralleled devices when compared to Case A. In this case, the improvement in switching performance of VSI, reaped by paralleling two devices, results in superior VSI efficiency over NSI at 400 V and 800 V for higher load currents. At 1 pu, the efficiency of VSI employing 24 devices is higher than NSI by approximately 1% and 0.2% for the 400 V and 800 V powertrain ratings, respectively.

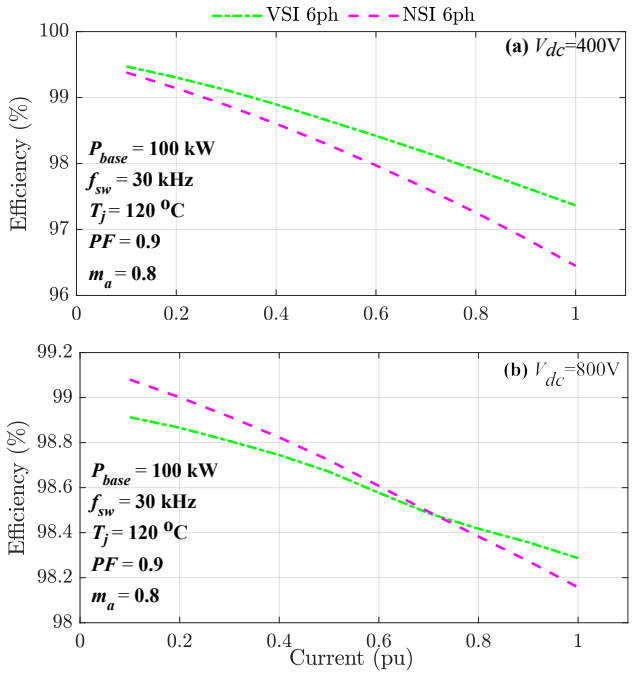

Fig. 6. Inverter efficiency evaluation with 36 and 24 devices at 400 V and 800 V bus, respectively, over load current sweep (nominal power 100 kW). (a) 400 Vdc. (b) 800 Vdc.

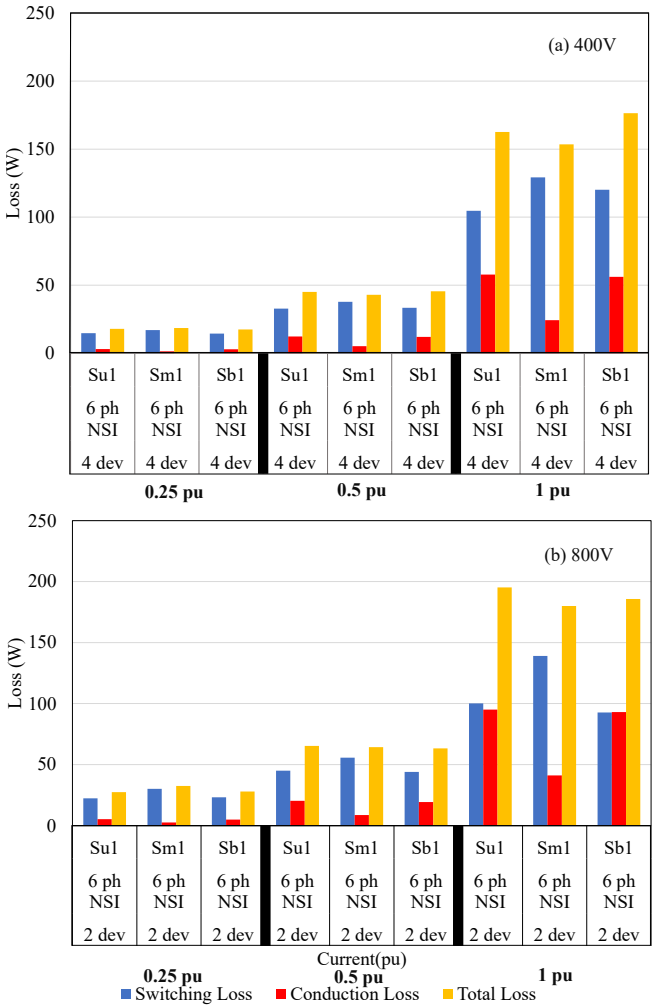

Fig. 7. Distribution of switching, conduction and total loss at S_u,S_b and S_m at three different load currents with 4 and 2 devices at 400 V and 800 V bus respectively per switch position. (a) 400 Vdc. (b) 800 Vdc.

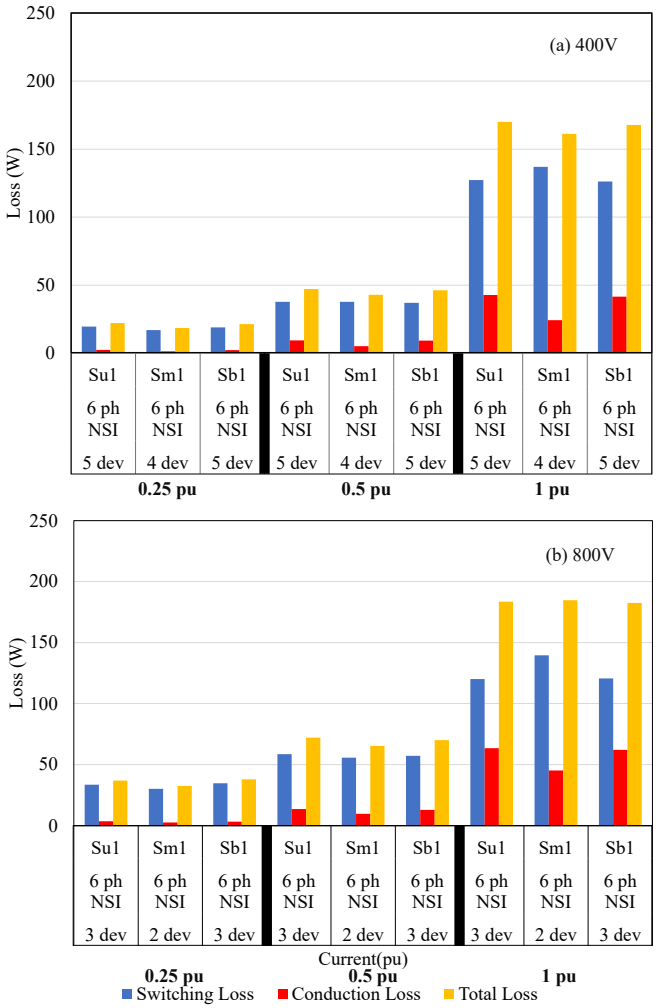

Fig. 8. Distribution of switching, conduction and total loss at S_u,S_b and S_m at three different load currents with 5,4,5 and 3,2,3 devices at 400 V and 800 V bus respectively every switching position. (a) 400 Vdc. (b) 800 Vdc.

Since the duty cycle of S_m in NSI operating in CF mode is considerably smaller than that of S_u and S_b, the resulting loss distribution profile is heterogeneous [10], with S_m dissipating energy at a much lower rate. This in turn complicates the design of a proper thermal management system. To overcome this issue at 400 V, five paralleled devices for the S_u and S_b NSI switches is considered, while S_m employs four paralleled devices. Similarly, at 800 V, three paralleled devices for the S_u and S_b NSI switches positions and two paralleled devices for the position S_m is used, the uneven device distribution per switch position in NSI is intended to balance the loss distribution among all devices and avoid hot spots. The resulting total device count in NSI is 36 and 24 for the 400 V and 800 V powertrains, respectively. Thus, the total device count in this case is equal in both topologies. Table II summarizes the relative efficiency of both topologies in all cases investigated. Generally, increasing the number of paralleled devices yields higher efficiency for both topologies. The next subsection investigates loss distribution per device in NSI. The same is not discussed for VSI because loss distribution is homogeneous across all switches.

B. Loss Distribution

Fig. 7 depicts the conduction and switching loss per device in NSI employing four and two paralleled devices per switch position (Cases A and B) at different operating points. For the 400 V powertrain (Fig. 7a), the switching loss in S_u and S_b is lower than that of S_m. However, the conduction loss is almost twice as high for S_u and S_b. For the 800 V powertrain (Fig. 7b), S_m exhibits a much lower conduction loss and higher switching loss when compared to S_u and S_b. It is noted that the losses at S_u and S_b scale in proportion with the S_m, as shown in Fig. 7b. Furthermore, with the increase in dc-bus voltage, the switching loss increases while the conduction loss is reduced. Thus, the uneven nature of the total loss distribution among devices in NSI is observed.

As explained earlier, one additional device is paralleled at S_u and S_b to offset the high conduction loss incurred by

them. Fig. 8 depicts the conduction and switching loss per device in NSI employing four paralleled devices in S_m and five paralleled devices in S_u and S_b for the 400 V powertrain (Fig. 8a), the conduction losses in S_u and S_b are still marginally higher when compared to S_m. On the other hand, the switching losses of S_u and S_b are lower when compared to the middle switch, S_m. Thus total loss at the three switch positions are now fairly uniform. For the 800 V powertrain two paralleled devices in S_m and three paralleled devices in S_u and S_b are used. (Fig. 8b) depicts higher switching loss but lower conduction loss as observed in S_u and S_b when compared to the loss distribution in Fig. 8a, at 800 V. The reduction in conduction loss and increase in switching loss is reaped from the additional devices at S_u and S_b, however as before we observe uniform total losses at the three switch positions. It can, therefore, be concluded that asymmetric paralleling of devices to counteract the heterogeneous loss distribution could be a feasible approach. Its effectiveness is more compelling for higher dc-bus voltage as the configuration yields higher efficiency when compared to the VSI at loads up to 0.7 pu.

IV. Conclusion

This study presented a comprehensive efficiency evaluation for two SiC-based six-phase inverter topologies (i.e. VSI and NSI) for automotive applications. Additionally, the total device count in NSI was compared to that of its VSI counterpart. Analysis based on minimum total device count, for cost optimization, demonstrated that NSI, more often than not, employs more devices for high power applications. This finding challenges the common narrative that NSI enjoys reduced number of devices.

The efficiency of both topologies was evaluated for 400 V and 800 V EV powertrains. Different cases of device paralleling in both topologies were also investigated. It was found that NSI can outperform VSI at 800 V powertrain voltage at loads of up to 0.7 pu and 100 kW of output power when utilizing the same device count.

References

[1] L. Ulrich, "Top 10 tech cars: The trend towards all-electric is accelerating," *IEEE Spectr.*, vol. 58, no. 4, pp. 44–53, Apr. 2021.

[2] C. McKerracher *et al.*, "Electric vehicle outlook 2020," BloombergNEF, Tech. Rep. EVO20, 2020. [Online]. Available: https://about.bnef.com/electric-vehicle-outlook/

[3] A. Emadi, "Transportation 2.0," *IEEE Power Energy Mag.*, vol. 9, no. 4, pp. 18–29, Jul. 2011.

[4] A. Salem and M. Narimani, "A review on multiphase drives for automotive traction applications," *IEEE Trans. Transp. Electrif.*, vol. 5, no. 4, pp. 1329–1348, Dec. 2019.

[5] E. Levi, F. Barrero, and M. J. Duran, "Multiphase machines and drives-revisited," *IEEE Trans. Ind. Electron.*, vol. 63, no. 1, pp. 429–432, Jan. 2016.

[6] E. Sayed, M. Abdalmagid, G. Pietrini, N.-M. Sa'adeh, A. D. Callegaro, C. Goldstein, and A. Emadi, "Review of electric machines in more/hybrid/turbo electric aircraft," *IEEE Trans. Transp. Electrif.*, pp. 1–1, Jun 2021.

[7] "TM4 SUMO^{TM} MD Motor / Inverter System," DANA TM4, Brochure CVTM4-DI002-0420, 2020. [Online]. Available: https://www.danatm4.com/wp-content/uploads/2019/04/TM4-SUMO-MD_Dana-TM4.pdf

[8] A. K. Morya, M. C. Gardner, B. Anvari, L. Liu, A. G. Yepes, J. Doval-Gandoy, and H. A. Toliyat, "Wide bandgap devices in AC electric drives: Opportunities and challenges," *IEEE Trans. Transp. Electrif.*, vol. 5, no. 1, pp. 3–20, Mar. 2019.

[9] W. Taha, "Comparative study on silicon carbide (SiC) polytypes in high voltage devices," in *2021 Int. Conf. Sustain. Energy Futur. Electr. Transport. (SeFeT)*, Hyderabad, 2021, pp. 1–6.

[10] C. Liu, B. Wu, N. Zargari, D. Xu, and J. Wang, "A novel three-phase three-leg AC/AC converter using nine IGBTs," *IEEE Trans. Power Electron.*, vol. 24, no. 5, pp. 1151–1160, May 2009.

[11] L. Zhang, P. C. Loh, F. Gao, and F. Blaabjerg, "A cascaded online uninterruptible power supply using reduced semiconductor," in *2011 IEEE Energy Convers. Congr. Expo. (ECCE)*, Phoenix, AZ, 2011, pp. 3167–3172.

[12] S. M. Dehghan, M. Mohamadian, and A. Yazdian, "Hybrid electric vehicle based on bidirectional Z-source nine-switch inverter," *IEEE Trans. Veh. Technol.*, vol. 59, no. 6, pp. 2641–2653, Jul. 2010.

[13] A. S. Salem, R. A. Hamdy, A. S. Abdel-Khalik, I. F. El-Arabawy, and M. S. Hamad, "Performance of nine-switch inverter-fed asymmetrical six-phase induction machine under machine and converter faults," in *2016 18th Int. Middle East Power Syst. Conf.*, Cairo, Dec. 2016, pp. 711–716.

[14] R. Wang, C. Li, C. Liu, C. Lu, and W. Wang, "Control strategy for four-leg nine-switch inverter under unbalanced loads," *IEEE Access*, vol. 8, pp. 50 377–50 389, Mar. 2020.

[15] E. C. dos Santos, C. B. Jacobina, and O. I. da Silva, "Six-phase machine drive system with nine-switch converter," in *IECON 2011 - 37th Annu. Conf. IEEE Ind. Electron. Soc.*, Melbourne, Nov. 2011, pp. 4204–4209.

[16] F. Gao, L. Zhang, D. Li, P. C. Loh, Y. Tang, and H. Gao, "Optimal pulsewidth modulation of nine-switch converter," *IEEE Trans. Power Electron.*, vol. 25, no. 9, pp. 2331–2343, Sep. 2010.

[17] N. Jarutus and Y. Kumsuwan, "A carrier-based phase-shift space vector modulation strategy for a nine-switch inverter," *IEEE Trans. Power Electron.*, vol. 32, no. 5, pp. 3425–3441, May 2017.

[18] X. Li, L. Qu, B. Zhang, G. Zhang, and H. Liao, "A simplified modulation strategy of nine-switch inverter to cut off half of switching modes," *IEEE Access*, vol. 6, pp. 7254–7261, Mar. 2018.

[19] J. Zhang, Y. Pang, K. Wang, D. Xu, and L. Pan, "Modulation method for nine-switch converter based on equivalent mechanism between nine-switch converter and dual six-switch converters," *IEEE Trans. Ind. Electron.*, vol. 68, no. 4, pp. 2845–2855, Apr. 2021.

[20] F. C. de Andrade, F. Bradaschia, L. R. Limongi, and M. C. Cavalcanti, "A reduced switching loss technique based on generalized scalar PWM for nine-switch inverters," *IEEE Trans. Ind. Electron.*, vol. 65, no. 1, pp. 38–48, Jan. 2018.

[21] J. Reimers, L. Dorn-Gomba, C. Mak, and A. Emadi, "Automotive traction inverters: Current status and future trends," *IEEE Trans. Veh. Technol.*, vol. 68, no. 4, pp. 3337–3350, Apr. 2019.

[22] J. Jenkins. (2020) Here's why tesla transitioned to a semi-custom power module design in model 3 inverter. CHARGED Electric Vehicles Mag. [Online]. Available: https://chargedevs.com/features/heres-why-tesla-transitioned-to-a-semi-custom-power-module-design-in-model-3-inverter/

[23] C. Zhao, L. Wang, X. Yang, F. Zhang, and Y. Gan, "Comparative investigation on paralleling suitability for SiC MOSFETs and SiC/Si cascode devices," *IEEE Trans. Ind. Electron.*, pp. 1–1, 2021.

[24] Z. Nie and N. Schofield, "Multi-phase vsi dc-link capacitor considerations," *IET Electr. Power Appl.*, vol. 13, no. 11, pp. 1804–1811, Mar. 2019.

[25] T. Kominami and Y. Fujimoto, "Inverter with reduced switching-device count for independent AC motor control," in *IECON 2007 - 33rd Annu. Conf. IEEE Ind. Electron. Soc.*, Taipei, 2007, pp. 1559–1564.

[26] I. López, E. Ibarra, A. Matallana, J. Andreu, and I. Kortabarria, "Next generation electric drives for HEV/EV propulsion systems: technology, trends and challenges," *Renew. Sustain. Energy Rev.*, vol. 114, p. 109336, Oct. 2019.

[27] W. Taha, B. Nahid-Mobarakeh, and J. Bauman, "Efficiency evaluation of 2L and 3L SiC-based traction inverters for 400V and 800V electric vehicle powertrains," in *2021 IEEE Transport. Electrific. Conf. Expo (ITEC)*, Chicago, IL, 2021, pp. 625–632.